Extended Abstracts of the 2008 International Conference on Solid State Devices and Materials, Tsukuba, 2008, pp. 1148-1149

J-7-2

Study of Fluorine Incorporation in the Blocking Oxide of Metal-Alumina-Nitride-Oxide-Silicon-type Flash Memory Devices

Man Chang, Joonmyoung Lee, Yongkyu Ju, Seungjae Jung, Hyejung Choi and Hyunsang Hwang

Department of Materials Science and Engineering, Gwangju Institute of Science and Technology,
261 Cheomdan-gwagiro (Oryong-dong), Buk-gu, Gwangju 500-712 Republic of Korea
Phone: +82-62-970-2380, Fax: +82-62-970-2304, e-mail: hwanghs@gist.ac.kr

Introduction

The blocking oxide serves to prevent the electron injections from the gate electrode during erase operations for metal-alumina-nitride-oxide-silicon (MANOS)-type flash memory devices. If the blocking oxide has many defect-related traps, it can lead to charge loss paths and interfere with the removal of trapped charges during an erase operation [1]. Thus, it may be necessary to optimize the quality of the blocking oxide. As a passivation method for decreasing defective bonds or traps in high-k dielectric, fluorine ambient has been intensively studied [2, 3]. It was reported that appropriate fluorine can successfully passivate the bulk oxygen vacancies in high-k oxide and defective bonds at the interface. However, the excessive fluorine causes degradation in electrical properties [4].

In this study, the effect of high-pressure fluorine annealing on the memory properties of MANOS-type flash memory is investigated.

Experimentals

After standard cleaning of a p-type Si wafer, a 4 nm thick SiO_2 was thermally grown for the tunnel oxide. A 7 nm thick Si_xN_y as a charge trapping layer was deposited by means of LPCVD. For the blocking oxide, a 15 nm thick Al_2O_3 layer was deposited by means of ALD. Subsequently, RTA was performed in an N_2 ambient for densification (denoted by 'NO HPFA'). For comparisons, some of NO HPFA samples were annealed in high-pressure fluorine ambient (denoted by 'HPFA'). The low temperature and high pressure are more suitable for the prevention of the growth of an interfacial layer [5]. For a metal electrode, Pt was deposited by means of an rf sputtering system. Finally, FG annealing was performed. The process conditions are shown in more detail in Fig. 1.

Results & Discussion

Fig. 2 shows the change of the capacitance of ONA stacks after 0.04 % and 0.21 % HPFA. There is no degradation of capacitance after HPFA. The negative shifts of V_{FB} are observed. This might be due to a removal of negative fixed charges and the passivation of oxygen vacancies in the bulk Al_2O_3 by HPFA [6, 7]. The interfacial layers (IL) between Al_2O_3 and Si_3N_4 for both samples are apparently observed by HR-TEM analysis (Fig. 3). The difference of IL thickness after 0.04% HPFA is negligible and its IL thickness is approximately 20~25 Å. To confirm fluorine incorporation, an XPS depth profile analysis was conducted (Fig. 4). Clearly, fluorine is distributed only in Al_2O_3 layer. The corresponding XPS spectrum at 686.5 eV indicates AlF_x peak, as shown in the inset of Fig. 4 [8]. Thus, it is concluded that HPFA replaces Al-O bonds with Al-F bonds in the Al_2O_3. Fig. 5 reveals the shift of Al 2p toward higher bonding energy near the Al_2O_3/Si_3N_4 IL after HPFA. These peaks were extracted from Fig. 4 at the same etching time, corresponding to the near interface region. This might be attributed to the dissociated oxygen from Al-O bonds by fluorine. This could be expressed as follows [9]:

$$Al_2O_3 + 3F_2 \rightarrow 2AlF_3 + 3/2O_2$$

Although the signals can be mixed by sputter process, the comparisons through XPS spectra can presumably be expected to give the information about the effect of HPFA, considering the low sputter rate (approximately 0.22 Å/s) and thick interfacial layer (T_{IL}~2.5 nm). Fig. 6 and 7 show the leakage current of MANOS devices and single Al_2O_3 MIS capacitors before/or after HPFA process, respectively. At high field region of HPFA samples, the reduced leakage current is observed (fig. 6 (c)). This can be explained by the reduction of oxygen vacancies and passivation of trap sites. However, 0.21 % HPFA sample shows the decrease of breakdown voltage because of excessive fluorine in Al_2O_3. Unexpectedly, the increases of leakage current for HPFA samples are observed at the middle region (fig. 6 (b)). This could be due to the decrease of tunneling distance by the reduced band bending, which can be induced by removal of fixed charges by fluorine passivation. This result is similar with that of single Al_2O_3 layer (Fig. 7).

The erase speed for HPFA samples is significantly enhanced at high voltage because of its improved blocking efficiency (Fig. 8). After applying -20 V for 1 sec, the differences of the $\triangle V_{FB}$ are -7.09 V, -8.48 V and -9.53 V for the NO HPFA, 0.04 % and 0.21 % HPFA samples, respectively. However, the program speed is not greatly improved (inset of Fig. 8). After 10^4 P/E cycling, 0.04 % and 0.21 % HPFA samples show larger memory windows (1.2 and 0.91 V) than that of NO HPFA sample (0.5 V). At retention characteristic at 160 ^oC (Fig. 10), 0.04% HPFA sample exhibits a lower charge loss rate (0.057 V/s) than that of NO HPFA sample (0.079 V/s). Furthermore, as the retention temperature increases, the difference of charge loss rate also increases (Fig. 11).

Summary

The effect of HPFA on MANOS-type flash memory devices was investigated. HPFA replaces Al-O bonds with Al-F bonds in the Al_2O_3, which reduces the oxygen vacancies and trap sites in the blocking oxide. As a result, the fluorine incorporation causes the blocking efficiency to improve and enhances such factors as the erase speed, endurance and retention characteristics of MANOS devices.

Acknowledgments

This work was supported by the National Program for Tera-Level Nano-devices through the Ministry of Education, Science and Technology (MEST), Korea.

References

[1] M. Chang et al., APL, 91, p192111 (2007)
[2] K. I. Seo et al., IEDM 2005, p429
[3] K. Tse et al., APL, 89, p142914 (2006)
[4] L. Tsetseris et al., APL, 85, p4950 (2004)
[5] P. Punchaipetch et al., JJAP, 45, pL120 (2006)
[6] C. S. Lai et al., ISDRS 2005, p266
[7] K.Torii et al., VLSI 2002, p188
[8] K.-H et al. Surf. Interface Anal., 21, p691 (1994)

- 4 nm thermally grown SiO_2 (850℃ in an O_2 ambient)
- 7 nm LPCVD Si_xN_y (730 ℃ with a gas flow ratio of SiH_2Cl_2/NH_3 = 0.13)
- 15 nm ALD Al_2O_3 (350 °C, TMA+$Al(CH_3)_3$+O_3)
- N_2 RTA at 1000 ℃ for 1 min
- Fluorine annealing (400 ℃, 10 atm, 20 min, 0.04 % and 0.21 % Ar/F_2 mixture gas)
- RF sputter Pt metal electrode
- FG annealing (400 ℃, 30 min)

Fig. 1 The fabrication process flow chart of MANOS devices

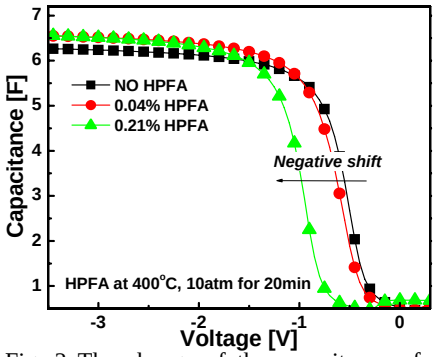

Fig. 2 The change of the capacitance of MANOS devices after 0.04 % and 0.21 % HPFA

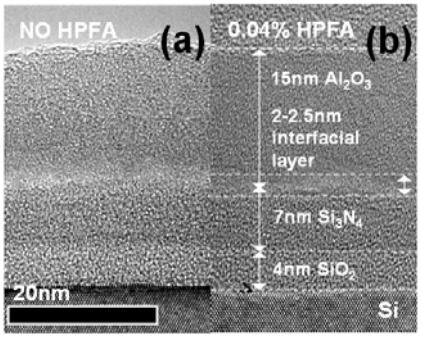

Fig. 3 Cross-sectional TEM images (a) NO HPFA sample (b) 0.04 % HPFA sample

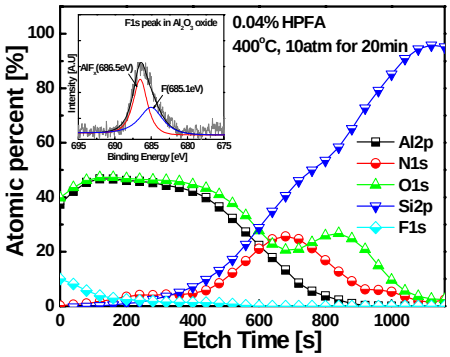

Fig. 4 XPS depth profile analysis and XPS spectra of F 1s in Al_2O_3 after 0.04 % HPFA (inset figure)

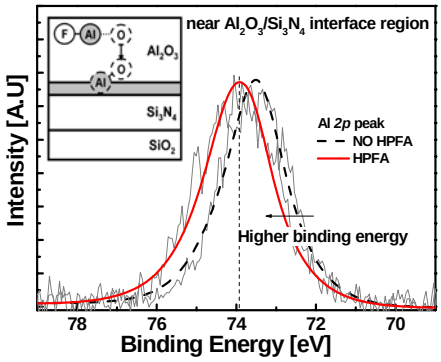

Fig. 5 XPS spectra of Al 2p near the Al_2O_3/Si_3N_4 interface layer region and a physical model of fluorine passivation

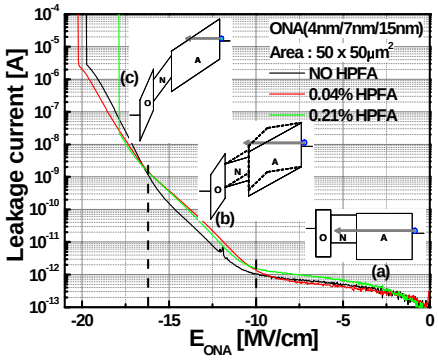

Fig. 6 The leakage current of MANOS devices after 0.04 % and 0.21 % HPFA and corresponding energy band diagrams

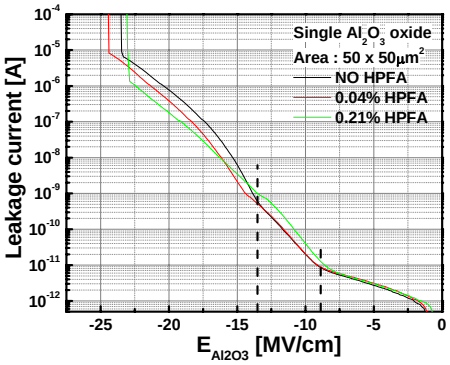

Fig. 7 The leakage current of single Al_2O_3 MIS capacitors after 0.04 % and 0.21 % HPFA

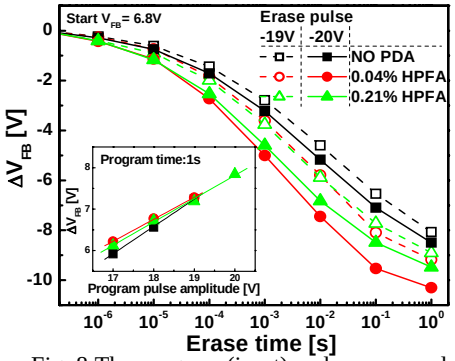

Fig. 8 The program (inset) and erase speed characteristics after 0.04 % and 0.21 % HPFA

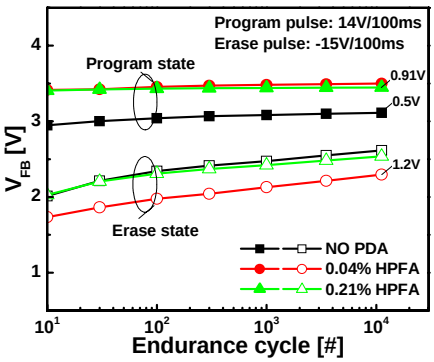

Fig. 9 Endurance characteristics of NO HPFA, 0.04 % and 0.21 % HPFA samples

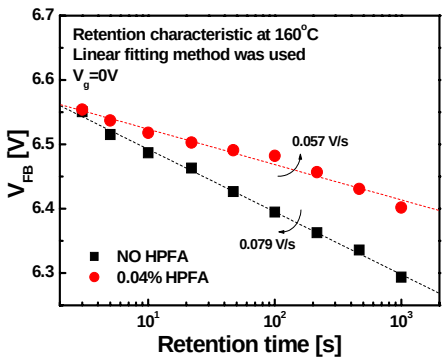

Fig. 10 The retention characteristics of NO HPFA and 0.04 % HPFA samples at 160°C

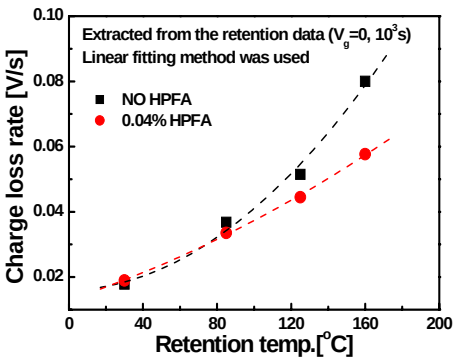

Fig. 11 The charge loss rates as a function of temperature of NO HPFA and 0.04 % HPFA samples